

## Supporting Information

### Multi-layered hybrid perovskites templated with carbazole derivatives: optical properties, enhanced moisture stability and solar cell characteristics

Roald Herckens<sup>a,†</sup>, Wouter T.M. Van Gompel<sup>a,†</sup>, Wenya Song<sup>b,c</sup>, María C. Gélvez-Rueda<sup>d</sup>, Arthur Maufort<sup>a</sup>, Bart Rutters<sup>e</sup>, Jan D'Haen<sup>e,f</sup>, Ferdinand C. Grozema<sup>d</sup>, Tom Aernouts<sup>b</sup>, Laurence Lutsen<sup>a,e</sup>, Dirk Vanderzande<sup>a,e,\*</sup>

<sup>a</sup>Hasselt University, Institute for Materials Research (IMO-IMOMEC), Hybrid Materials Design (HyMaD), Martelarenlaan 42, B-3500 Hasselt, Belgium.

<sup>b</sup>imec, Thin-Film Photovoltaics, Energyville, Thor Park 8320, B-3600 Genk, Belgium.

<sup>c</sup>KU Leuven, ESAT, B-3001 Leuven, Belgium.

<sup>d</sup>Delft University of Technology, Department of Chemical Engineering, Section Optoelectronic Materials, Van der Maasweg 9, 2629 HZ Delft, The Netherlands.

<sup>e</sup>imec, Associated Laboratory IMOMEC, Wetenschapspark 1, B-3590 Diepenbeek, Belgium.

<sup>f</sup>Hasselt University, Institute for Materials Research (IMO-IMOMEC), Electrical and physical characterization (ELPHYC), Martelarenlaan 42, B-3500 Hasselt, Belgium.

<sup>†</sup>These authors contributed equally.

#### Synthesis of carbazole derivatives (CA-C<sub>4</sub>)

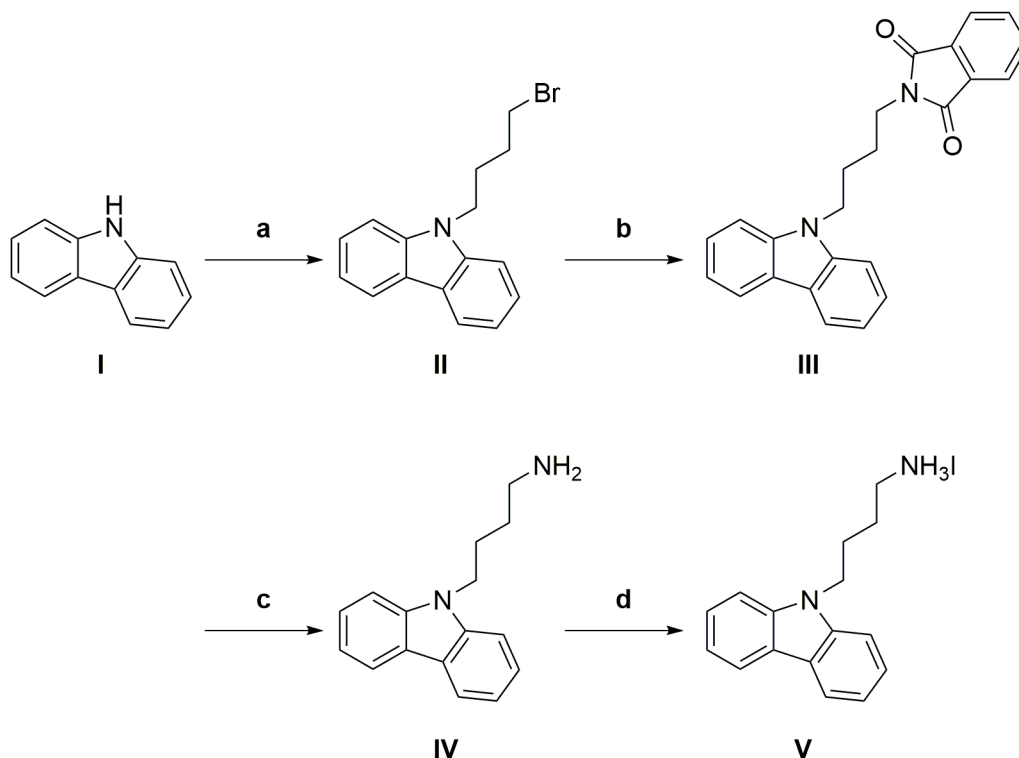


**Figure S1** a) 1,4-dibromobutane, KO-tBu, THF, 55 °C, 10h. b) Potassium phthalimide, DMF, 80 °C, 6h. c) Hydrazine monohydrate (65%), EtOH, 100 °C, 2h. d) HI, EtOH, RT.

9-(bromobutyl)-9H-carbazole (**II**): 1,4-dibromobutane (29.14 g, 135 mmol) was added dropwise to a mixture of 9H-carbazole (15.00 g, 90 mmol) and potassium tert-butoxide (10.07 g, 90 mmol) in tetrahydrofuran (THF, 130 mL). The reaction mixture was heated to 55 °C and stirred under nitrogen atmosphere for 10h. The reaction was followed with thin layer chromatography (TLC). After the reaction was completed, the mixture was allowed to cool down to room temperature and extracted with H<sub>2</sub>O (100 mL) and DCM (3x 45 mL). Next, the organic layer was dried with magnesium sulfate, filtered and the solvent was removed by vacuum elimination. The residue was purified by flash chromatography (DCM/Petroleum ether 1/5), to obtain **II** as a colorless solid (74.9%). <sup>1</sup>H NMR (400 MHz, Chloroform-d) δ 8.12 (dt, J = 7.7, 1.0 Hz, 2H), 7.48 (ddd, J = 8.2, 7.0, 1.2 Hz, 2H), 7.41 (dt, J = 8.2, 0.9 Hz, 2H), 7.25 (ddd, J = 7.9, 7.0, 1.1 Hz, 2H), 4.36 (t, J = 6.9 Hz, 2H), 3.39 (t, J = 6.5 Hz, 2H), 2.12 – 2.03 (m, 2H), 1.97 – 1.86 (m, 2H).

2-((9H-carbazol-9-yl)butyl)isoindoline-1,3-dione (**III**): potassium phthalimide (25.70 g, 139 mmol) was added to a solution of **II** (29.20 g, 97 mmol) in dimethylformamide (135 mL, DMF). The reaction mixture was heated to 80 °C and stirred for 6h. Afterwards, the mixture was allowed to cool down to room temperature and aqueous ammonium chloride and chloroform were added. Next, the reaction mixture was extracted with H<sub>2</sub>O (2x 100 mL) and saturated aqueous sodium chloride (2x 100 mL). The organic layer was dried with magnesium sulfate, filtered and the filtrate was evaporated by vacuum elimination. The residue was purified by column chromatography (Ethyl acetate/Hexane 1:5) and recrystallization (methanol) to obtain **III** as a colorless solid (77.6%). <sup>1</sup>H NMR (400 MHz, Chloroform-d) δ 8.09 (dt, J = 7.7, 1.0 Hz, 2H), 7.83 (dd, J = 5.4, 3.0 Hz, 2H), 7.70 (dd, J = 5.4, 3.0 Hz, 2H), 7.51 – 7.39 (m, 4H), 7.22 (ddd, J = 7.9, 6.7, 1.3 Hz, 2H), 4.36 (t, J = 7.0 Hz, 2H), 3.71 (t, J = 7.0 Hz, 2H), 2.02 – 1.88 (m, 2H), 1.84 – 1.73 (m, 2H).

(9H-carbazol-9-yl)butyl-1-amine (**IV**): Hydrazine monohydrate (65 wt. % in H<sub>2</sub>O, 6.24 mL, 129 mmol) was added to a refluxing solution of **III** (19.78 g, 53.7 mmol) in ethanol (500 mL) and reacted for 2h. Over the course of the reaction, large white crystals precipitate. After the reaction was completed, the reaction mixture was allowed to cool down to room temperature and the precipitate was filtered off and the solvent was removed by vacuum elimination. Next, the residue was dissolved in chloroform and again filtered. The filtrate was concentrated by rotary evaporation, to obtain **IV** (78.8%). <sup>1</sup>H NMR (400 MHz, Chloroform-d) δ 8.11 (dt, J = 7.8, 1.0 Hz, 2H), 7.47 (ddd, J = 8.2, 7.0, 1.2 Hz, 2H), 7.41 (dt, J = 8.3, 0.9 Hz, 2H), 7.23 (ddd, J = 8.0, 7.0, 1.1 Hz, 2H), 4.33 (t, J = 7.1 Hz, 2H), 2.69 (t, J = 7.1 Hz, 2H), 1.98 – 1.86 (m, 2H), 1.56 – 1.47 (m, 2H).

(9H-carbazol-9-yl)butyl-1-ammonium iodide (**V**): Hydrogen iodide was generated in situ and added to a solution of **IV** in ethanol at room temperature. Afterwards, the solvent was evaporated. Next, the residue was redissolved in ethanol and precipitated in a large amount of cooled ether. The residue was further purified by recrystallization in ethanol to obtain **V** as a colorless solid. <sup>1</sup>H NMR (400 MHz, DMSO-d<sub>6</sub>) δ 8.16 (dt, J = 7.7, 1.0 Hz, 2H), 7.63 (dt, J = 8.2, 0.8 Hz, 2H), 7.54 (s, 3H), 7.46 (ddd, J = 8.3, 7.1, 1.2 Hz, 2H), 7.20 (ddd, J = 7.9, 7.1, 0.9 Hz, 2H), 4.45 (t, J = 6.8 Hz, 2H), 2.77 (t, J = 7.6 Hz, 2H), 1.89 – 1.78 (m, 2H), 1.62 – 1.46 (m, 2H).

## Supporting figures

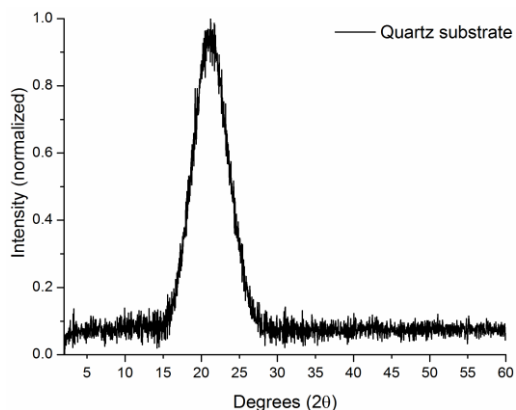


**Figure S2** X-ray diffraction pattern of a quartz substrate.

**Table S1** Calculation of the interplanar spacing for CA-C<sub>4</sub>  $n = 1$  based on Figure 1.

$2\theta$	$\theta$	n (reflection order)	$\sin(\theta)$		d (interplanar spacing in nm)	$\lambda = 0.15418 \text{ nm}$
3.45	1.73	1	0.03		2.56	
6.95	3.48	2	0.06		2.54	
10.40	5.20	3	0.09		2.55	
13.95	6.98	4	0.12		2.54	
17.40	8.70	5	0.15		2.55	
				Average	2.55 nm	<b>25.5 Å</b>

**Table S2** Calculation of the interplanar spacing for CA-C<sub>4</sub>  $n = 2$  based on the  $\langle n \rangle = 2$  pattern in Figure 2.

$2\theta$	$\theta$	n (reflection order)	$\sin(\theta)$		d (interplanar spacing in nm)	$\lambda = 0.15418 \text{ nm}$
2.91	1.46	1	0.03		3.04	
5.77	2.89	2	0.05		3.06	
8.59	4.30	3	0.07		3.09	
11.41	5.71	4	0.10		3.10	
14.31	7.16	5	0.12		3.09	
				Average	3.08 nm	<b>30.8 Å</b>

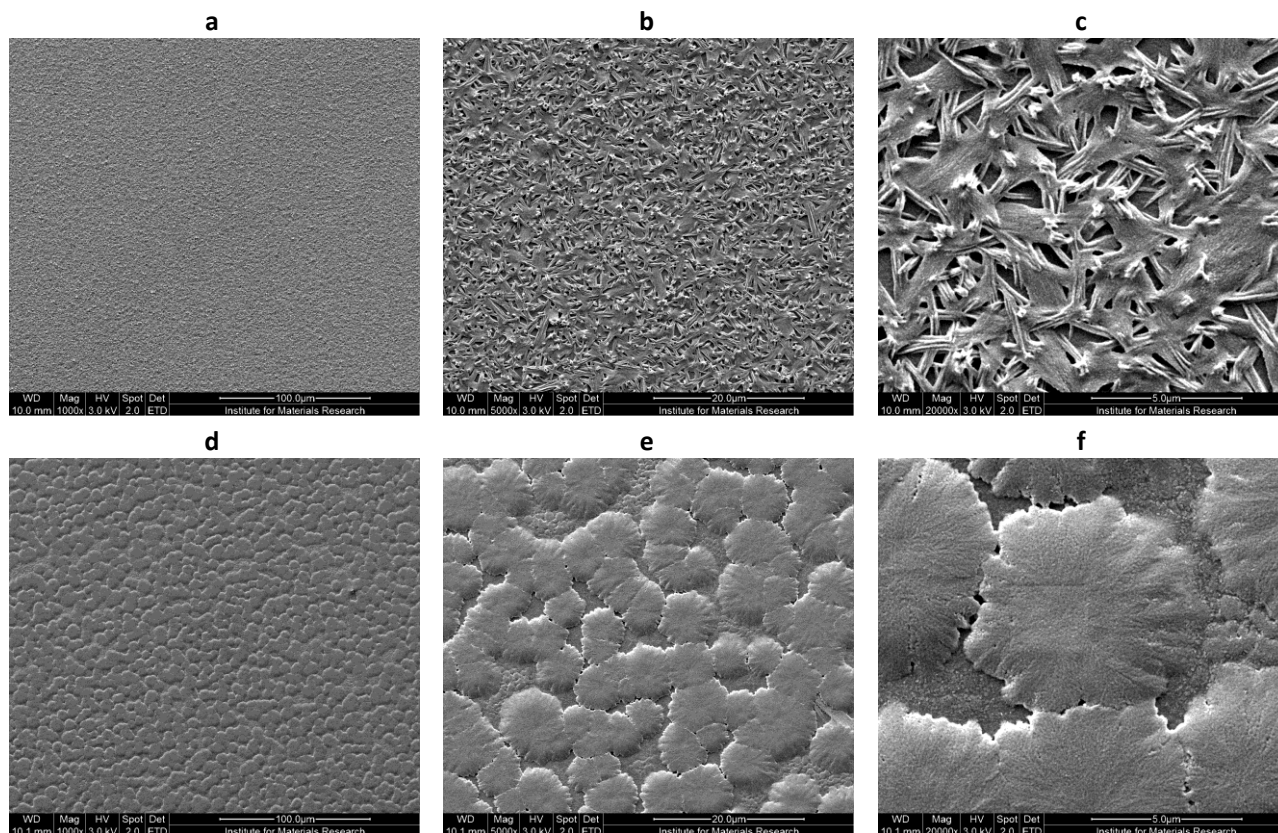


**Figure S3.** SEM pictures of spin-coated and post-annealed (a-c) and hot-cast (d-f) films of CA-C<sub>4</sub>  $\langle n \rangle = 40$ .

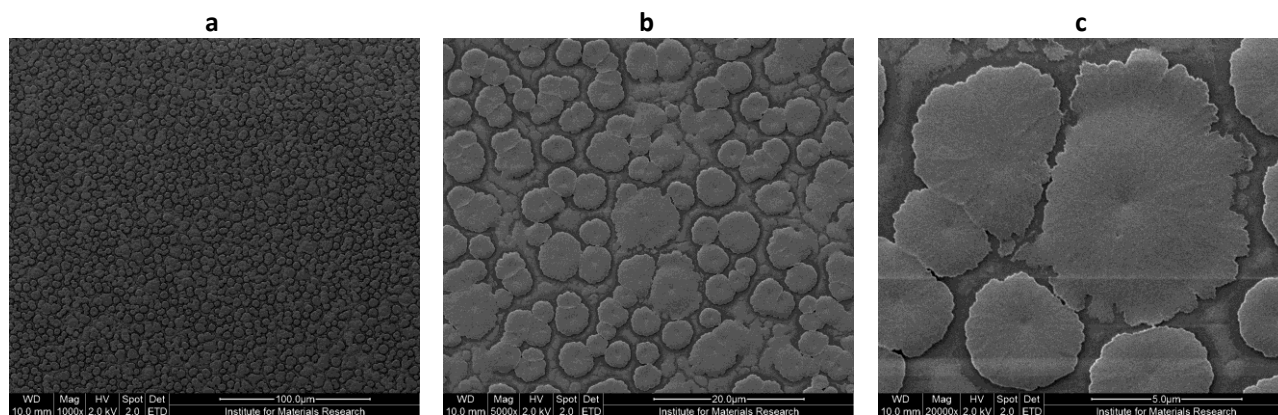


**Figure S4.** SEM pictures of hot-cast films of PEA  $\langle n \rangle = 40$  (a-c).

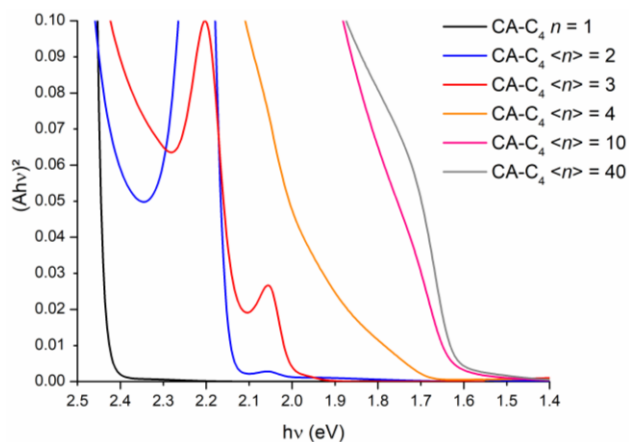


**Figure S5.** Zoom of Figure 3 in the main article to more clearly distinguish the absorption onsets.

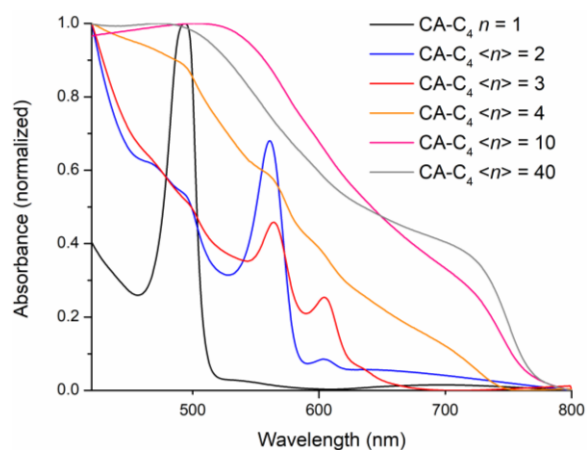


**Figure S6.** Absorption spectra (absorbance over wavelength) corresponding to the Tauc plots in Figure S3 in the main article.

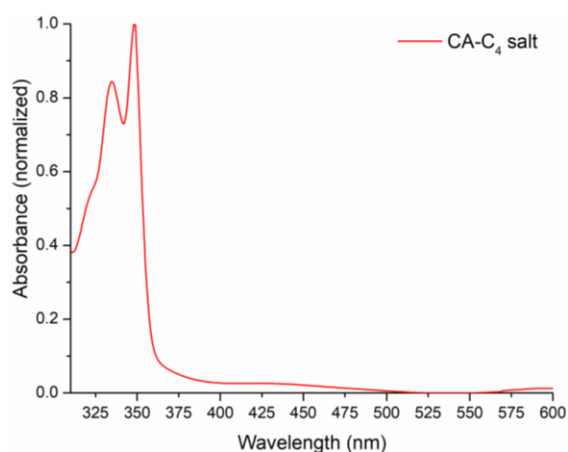


**Figure S7** Normalized absorption spectrum of a drop-casted film of the CA-C<sub>4</sub> precursor salt, dried at 110 °C for 15 min.

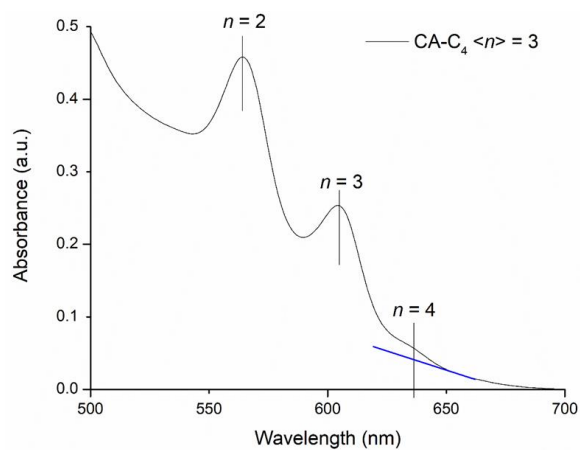


**Figure S8** Absorption spectrum of a CA-C<sub>4</sub> <n> = 3 film with the excitonic absorption peak positions assigned. The blue line is a guide to the eye.

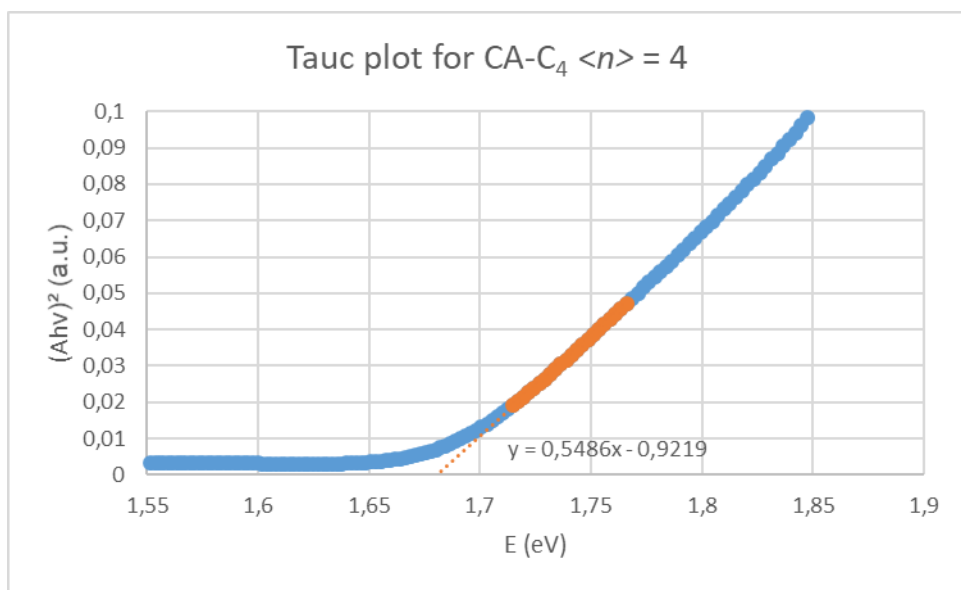


**Figure S9** Tauc plot for CA-C<sub>4</sub> <n> = 4 with a tangent intersecting the energy axis, as a representative plot. The formula for the tangent is shown in the plot.

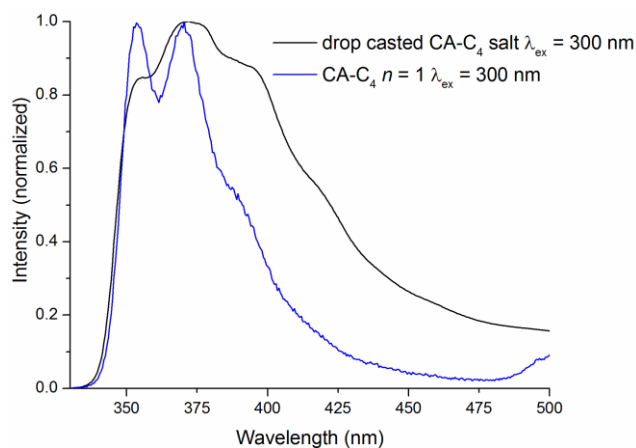


**Figure S10** Normalized photoluminescence emission spectra of a drop-casted film of the CA-C<sub>4</sub> precursor salt and a (CA-C<sub>4</sub>)<sub>2</sub>PbI<sub>4</sub> spin-coated film, both dried at 110 °C for 15 min, using an excitation wavelength of 300 nm.

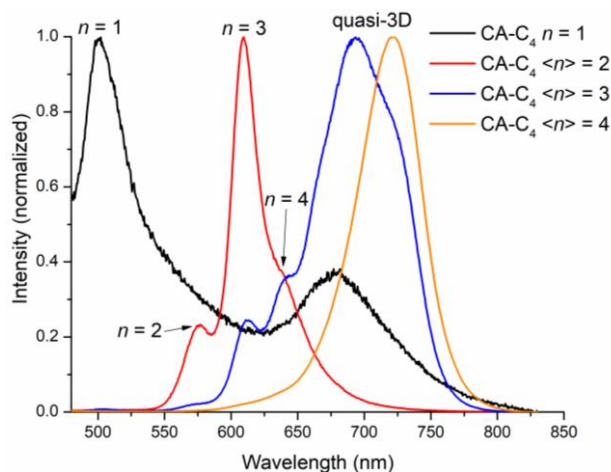


**Figure S11** Normalized photoluminescence emission spectra with the excitonic emission peaks assigned to a certain multi-layered perovskite ( $n$ ). The higher wavelength emission peaks are assigned to quasi-3D perovskites. See Table 4 of the article for the emission peak values of  $n = 1, 2, 3$  and 4. See Table 5 of the article for the emission peak values of these quasi-3D perovskites.

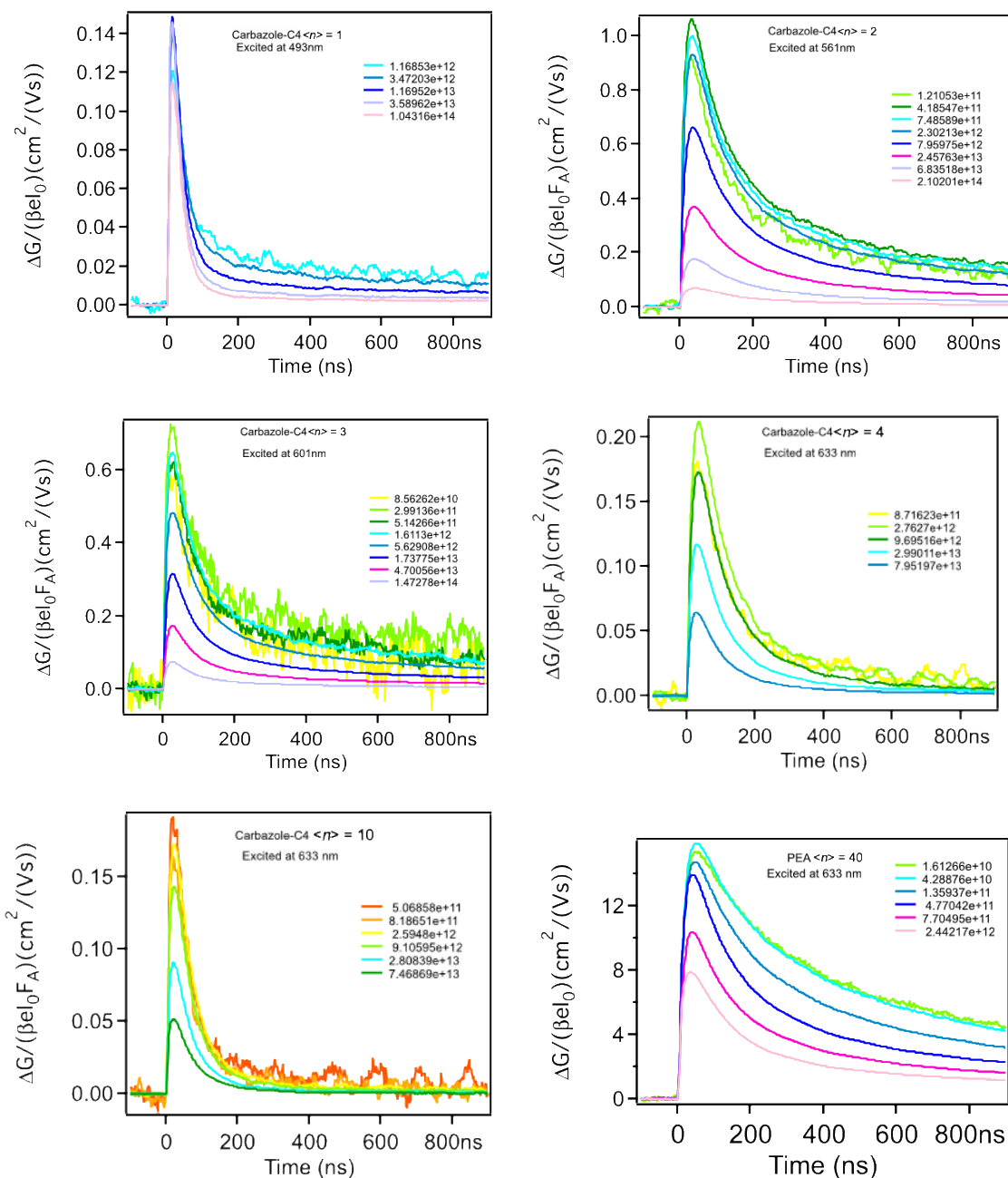


**Figure S12** Change of photo-conductivity as a function of time. Excited at 493 nm for CA-C4  $\langle n \rangle = 1$ , 561 nm CA-C4  $\langle n \rangle = 2$ , 601 nm for CA-C4  $\langle n \rangle = 3$ , 633 nm for CA-C4  $\langle n \rangle = 4$ , 10, 40 and PEA  $\langle n \rangle = 40$ .



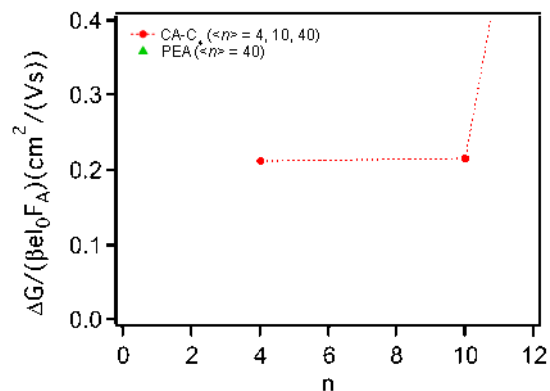


**Figure S13** Change of photo-conductivity as a function of  $\langle n \rangle$  ( $\langle n \rangle = 4, 10$ ). Excited at 633 nm for CA-C<sub>4</sub>  $\langle n \rangle = 4$  and 10. Samples were prepared by hot-casting at 110 °C.

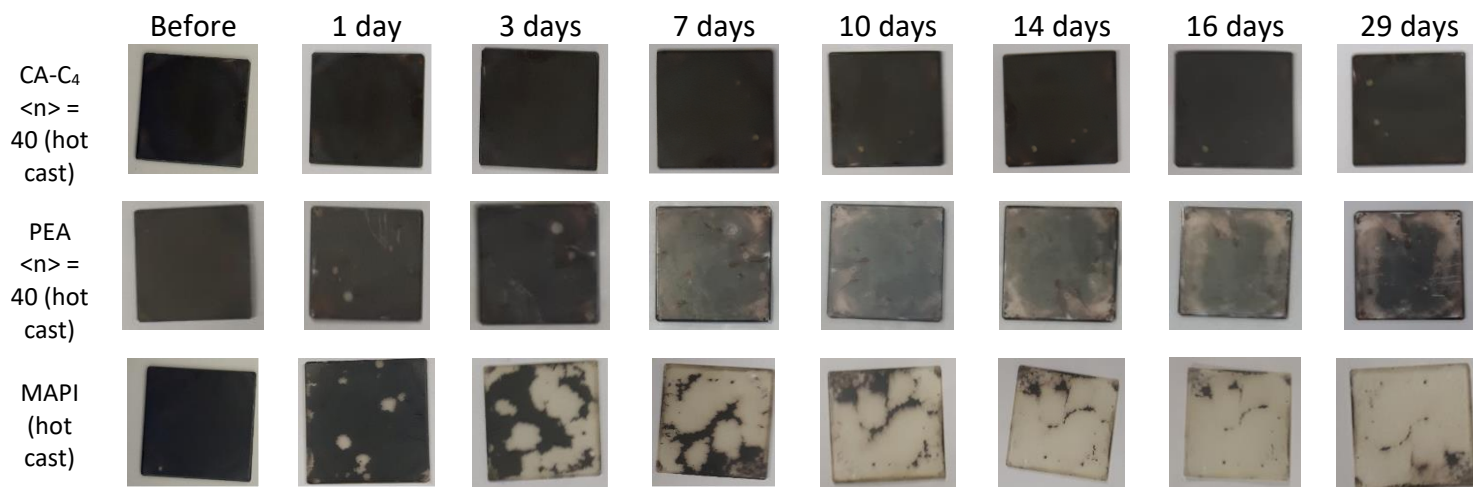


**Figure S14** Optical pictures of CA-C<sub>4</sub>  $\langle n \rangle = 40$  (top), PEA  $\langle n \rangle = 40$  (middle) and MAPbI<sub>3</sub> (bottom) films, hot-casted at 110 °C, after exposure to 77 % RH.

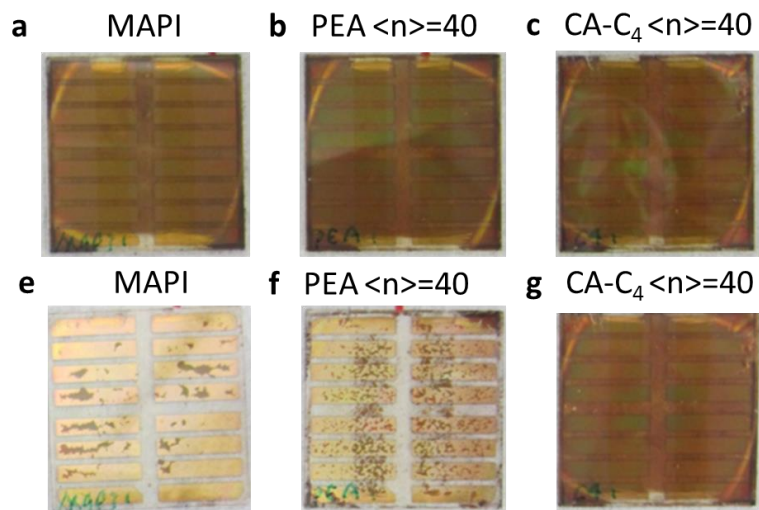


**Figure S15** Optical pictures of perovskite solar cells before (a-c) and after (e-g) being stored in 77 % RH air for 264 h.